# MECHANISM OF EARTH PRESSURE AND SIDEWALL FRICTION ACTING ON AN EMBEDDED FOOTING IN DRY SAND BASED ON CENTRIFUGE TESTING

**Shuji Tamura[1], Tadashi Sakamoto[2], Takenori Hida[3] and Nobuhiro Maeda[4]**

[1] *Associate Professor, Disaster Prevention Research Institute, Kyoto University, Kyoto Japan*
[2] *Researcher, Institute of Technology, Shimizu Corporation, Tokyo Japan*
[3] *Graduate student, Kyoto University, Kyoto Japan*
[4] *BayCurrent Consulting, Inc., Tokyo Japan*
*E-mail: tamura@sds.dpri.kyoto-u.ac.jp*

**ABSTRACT:**

Dynamic centrifuge testing of a superstructure-footing-piles model in dry sand deposit was performed, yielding the following conclusions. (1) Earth pressure and wall friction acting on the active and passive sides of the footing were investigated. The hysteresis loop shape of the relative displacement and the wall friction resembles that of the earth thrust. When the total earth thrust amplitude decreases, both sides' wall friction tends to act upward on the footing, suggesting that the earth pressure acting on both sides corresponds to the passive side. (2) The sidewall friction and earth pressure acting on the sidewalls of the footing were investigated. The sidewall friction amplitude increases with increasing relative displacement because the earth pressure amplitude increases with increasing relative displacement.

**KEYWORDS:** earth pressure, friction, embedded footing, piles, centrifuge model test, sand

## 1. INTRODUCTION

Lateral response of an embedded footing, such as that by earth pressure and friction, affects the pile stress occurring during an earthquake. Large-scale shaking table tests demonstrate that the lateral response decreases pile stress in non-liquefaction tests but increases pile stress in liquefaction tests (Tamura et al., 2005), which indicates that the evaluation of the lateral response of an embedded footing is important for the seismic design of pile foundations.

The relative contribution of the base, sidewall, and active and passive side of an embedded footing were evaluated based on cyclic lateral loading centrifuge tests (Garde and Dobry, 1998), reflecting that the contribution of the passive side accounts for more than half of the total lateral capacity of the footing. Earth pressure and sidewall friction acting on the embedded footing were investigated based on dynamic centrifuge tests on a superstructure-footing model supported on piles in dry sand deposits of different relative densities (Tamura et al., 2007). Results of this study show that the total earth pressure in the dense sand case plays an important role in reducing the shear force at pile heads because the difference between the total earth pressure and sidewall friction in the dense sand is greater than that in loose sand.

Wall friction is an important factor to evaluate passive earth pressure based on the Coulomb theory. Lateral earth pressure acting on sidewalls of an embedded footing is also important to evaluate the sidewall friction theoretically. However, knowledge of the wall friction and the lateral earth pressure during a large earthquake remain limited.

The objectives of this paper are: 1) to evaluate not only dynamic earth pressure but also wall friction acting on active/passive sides, 2) to evaluate dynamic friction and lateral earth pressure acting on sidewalls. For those purposes, dynamic centrifuge testing of a superstructure-footing-piles model in sand deposit was performed. Compressive and vertical forces acting on the active and passive sides of the embedded footing and shearing and compressive forces acting on the sidewalls were measured during the shaking.

## 2. CENTRIFUGE TESTS PERFORMED

### *2.1 Model Preparation*

Centrifuge tests were performed at 40 × *g* centrifugal acceleration using the geotechnical centrifuge at the Disaster Prevention Research Institute, Kyoto University. Figure 1 portrays a pile-footing-superstructure model prepared in a laminar shear box with inner dimensions of 450 mm (length) × 150 mm (width) × 200 mm (height). The soil model used for dry sand deposit was Toyoura sand ($D_{50}$=0.21 mm) with *Dr*=40%. A 2 × 2 pile model was used. The piles were modeled with an 8-mm-diameter and a 176-mm-long round aluminum bar. The bending stiffness, *EI* of the pile model was 142 kN·cm$^2$. A sketch and conditions of a pile-footing-superstructure model are depicted respectively in Fig. 2 and Table 1. The lid-shaped footing was modeled with rigid brass of 86 mm (shaking direction) × 64 mm (width) × 54 mm (height). The pile heads were linked rigidly to the upper plate of the footing; their tips were also linked rigidly to the laminar shear box. The strain gauges at the pile heads were not in contact with the soil. Four plates supported by small load cells were set up on the active and passive sides and shearing sides of the footing. The load cells were available for measurement in two different directions. Compressive and vertical forces acting on the active and passive sides of the embedded footing and shearing and compressive forces acting on the sidewalls were measured during the shaking. Plus and minus signs of each force were defined as depicted in Fig. 3.

The footing model surface is smoother than that of the prototype. Therefore, Toyoura sand was pasted on the active/passive sides and shearing sides of the footing. The footing was embedded 44 mm into the dry sand. The superstructure was modeled with rigid brass. The superstructure mass was 2.00 kg; that of the footing was 0.79 kg. The natural frequency of the superstructure under the fixed footing condition was about 105 Hz. Excitation

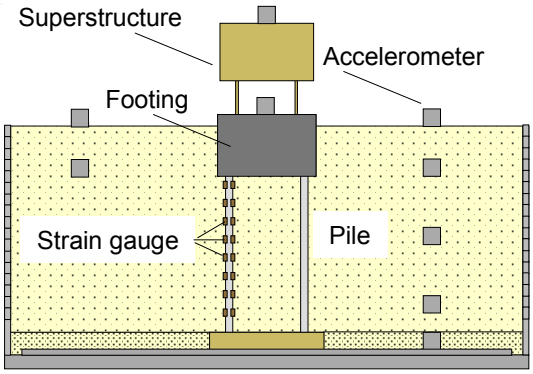


Figure 1 Test model

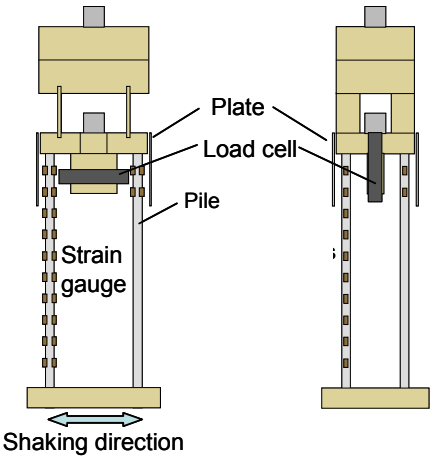


Figure 2 Piles-footing-superstructure model

Table 1 Conditions of piles-footing-superstructure system in prototype and model scale

| | | unit | Prototype | Model |
|---|---|---|---|---|
| Pile | Diameter | m | 0.32 | 0.008 |
| | *EI* | kNm$^2$ | $3.64\times10^{4}$ | $1.42\times10^{-2}$ |
| Footing | Mass | kg | 50,560 | 0.79 |
| | Length (L × B × H) | m | 3.44 × 2.56 × 2.16 | 0.086 × 0.064 × 0.054 |
| Structure | Mass | kg | 128,000 | 2.00 |
| | Natural frequency | Hz | 2.63 | 105 |

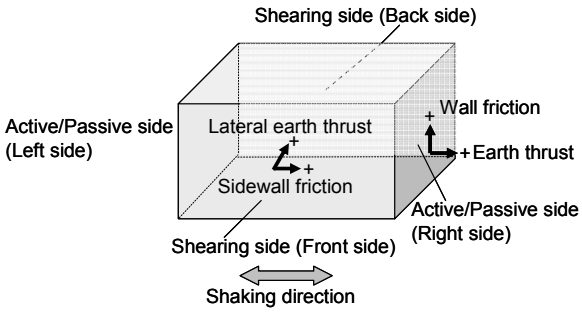


Figure 3 Definition of sign of forces acting on active/passive sides and side walls

for the test used Rinkai92, which is a synthesized ground motion for the Tokyo Bay area. All data presented in the following sections are of prototype scale.

### *2.2 Test results*

*2.1.1 Dynamic Response of the Soil-Pile-Superstructure System*

Figure 4 portrays the acceleration time histories of the superstructure, footing and ground surface, as well as those of input accelerations, the footing and ground surface displacement, the superstructure footing inertia defined by the sum of the superstructure and footing inertia, and the shear force defined by the sum of shear force at the pile heads. The shear force was evaluated through differentiation of the strain of the piles; the displacements were calculated according to the double integration of the accelerometer recordings. The amplitude of the footing acceleration is greater than that of the ground surface acceleration, probably because the footing response is affected by the superstructure response. The footing displacement amplitude is apparently larger than that of the ground surface displacement. The shear force is about half the amplitude of the superstructure footing inertia, suggesting that the lateral response of the embedded footing composed of earth pressure and friction reduced the shear force at the pile heads.

*2.1.2 Phase difference between lateral response of embedded footing and superstructure inertia*

To show effects of the lateral response of the embedded footing, the relation between the superstructure footing inertia $F_{is}$ and the total earth thrust $P_{et}$ defined by the difference between the active/passive sides earth pressure are shown in Figs. 5 and 6 along with the relation between the superstructure footing inertia and the sidewall friction $P_{fs}$ defined by the sum of side shear of the footing. The data in the first and third quadrants show that the lateral response tends to be in phase with the inertia force, although data in the second and fourth

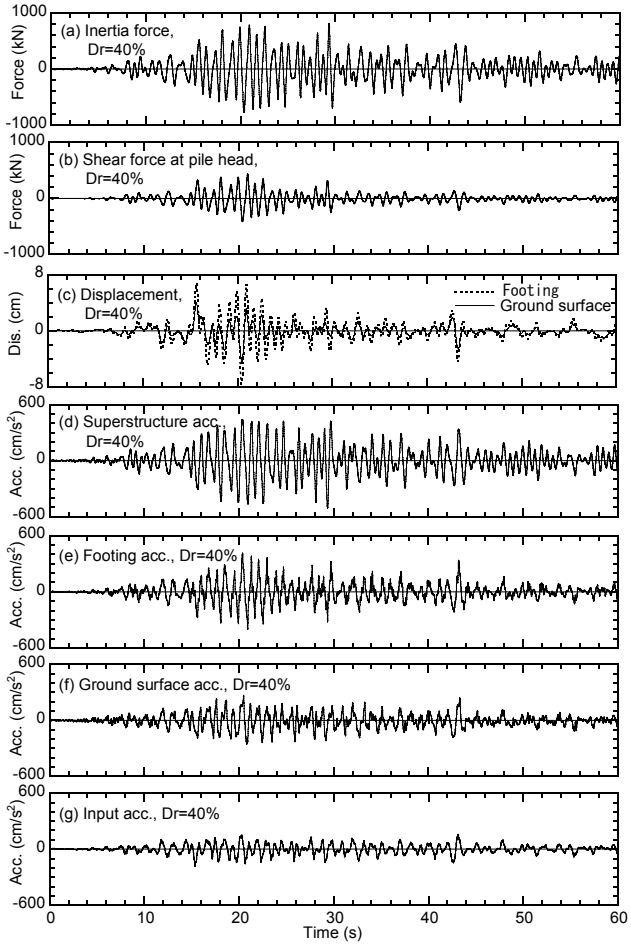


Figure 4 Time histories of inertia force, shear force, displacement and acceleration

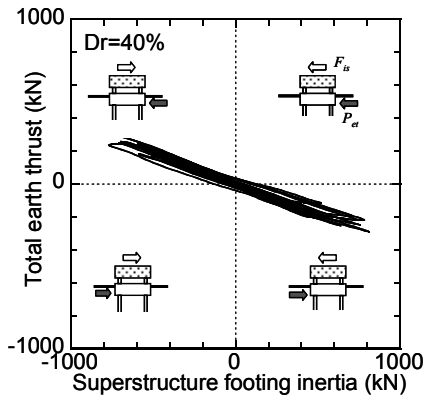


Figure 5 Relation between superstructure footing inertia and total earth thrust

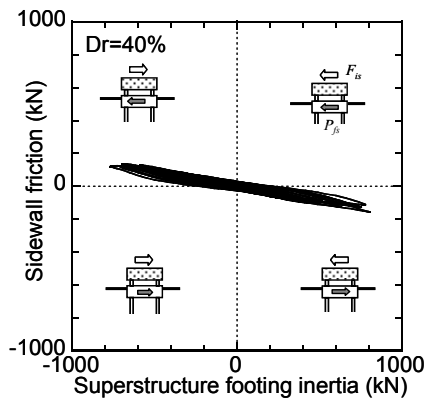


Figure 6 Relation between superstructure footing inertia and sidewall friction

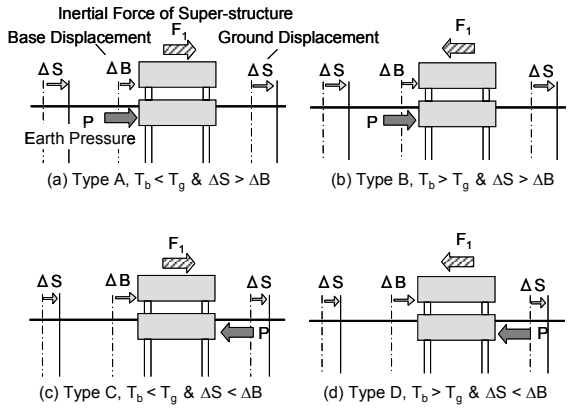


Figure 7 Phase between superstructure inertia and total earth thrust (Tamura et al. 2002)

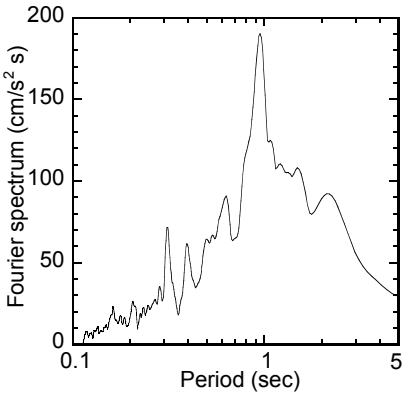


Figure 8 Fourier spectrum of ground surface acceleration

quadrants show that the lateral response tends to be out of phase by 180 deg with the inertial force. In Figs. 5 and 6, most test data are in the second and fourth quadrants; that fact indicates that the total earth thrust and the sidewall friction is out of phase with the superstructure footing inertia by 180 deg. Therefore, the amplitude of the shear force at pile heads is less than the superstructure footing inertia, as depicted in Fig. 4.

The phase difference between superstructure inertia and total earth thrust can be estimated by the natural period of the superstructure under the fixed footing condition $T_b$, the predominant period of the ground $T_g$, the soil displacement $\Delta S$, and the footing displacement $\Delta S$ (Tamura et al., 2002), as portrayed in Fig. 7. Figure 8 shows a Fourier spectrum of the ground surface acceleration. The predominant period of the ground is 0.95 (s), which is longer than the natural period of the superstructure. Considering that the footing displacement is greater than the soil displacement, Type C is estimated, indicating the total earth thrust tends to be out of phase by 180 deg with the superstructure inertia.

## 3. EARTH PRESSURE AND SIDEWALL FRICTION

### *3.1 Earth pressure and wall friction acting on active/passive side*

Figure 9 shows time histories of relative displacement between the ground surface and the footing, the total earth thrust, earth thrust, and wall friction of the right and left sides of the footing for $t$=20–30 s. The right and left sides of the footing tend to be passive and active sides, respectively when the sign of the relative displacement is plus. Peaks of the passive side earth pressure tend to be sharp, indicating that earth pressure does not reach a passive state. On the other hand, the peaks of the active side earth pressure tend to be dull, indicating that the earth pressure reaches the active state. The wall friction waveform resembles that of the earth thrust.

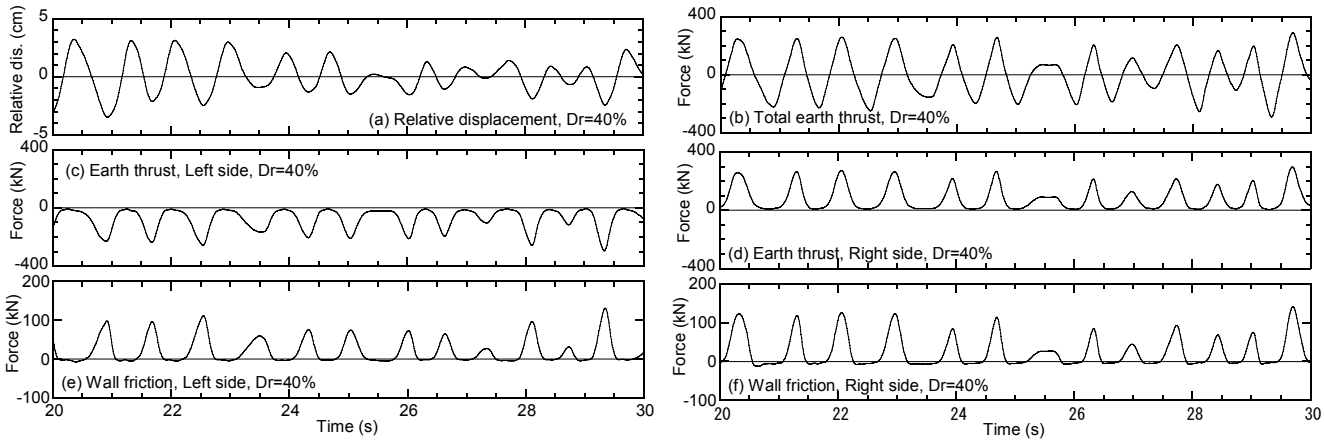


Figure 9 Time histories of relative displacement, total earth thrust, earth thrust of right and left sides of the footing and wall friction of right and left sides for t=20-30

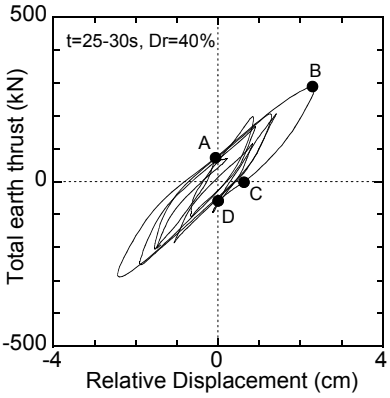


Figure 10 Relation between relative displacement and total earth thrust

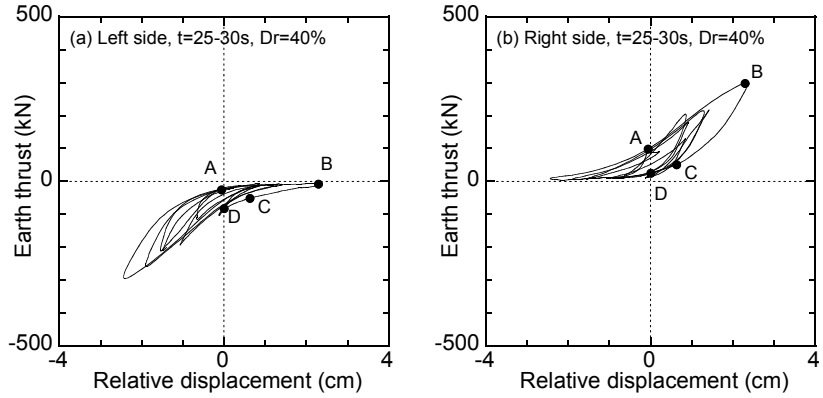


Figure 11 Relation between relative displacement and earth thrust

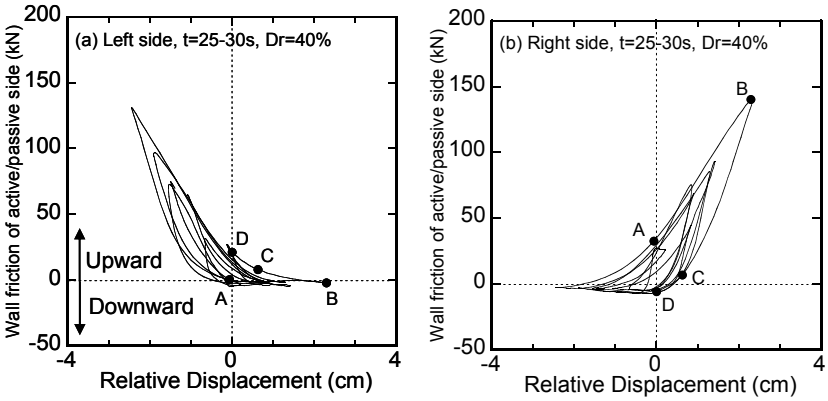


Figure 12 Relation between relative displacement and wall friction

The relation between the relative displacement and the total earth thrust is presented in Fig. 10. The hysteresis loops of the earth thrust and the wall friction acting on the right and left sides of the footing are also shown in Figs. 11 and 12 for $t$=25–30 s. The shape of the hysteresis loop of the wall friction resembles that of the earth thrust, except that the wall friction has both plus and minus signs. The wall friction acts upward or downward on the footing, whereas the earth pressure always acts as a compressive force on the footing.

The hysteresis loop of the total earth thrust is separable into three processes as depicted in the figure: A → B, B → C, and C → D. First, the total earth thrust during reloading A → B is caused mainly by earth pressure acting on the right side of the footing. The right side wall friction acts upward on the footing and increases rapidly. In contrast, the left side wall friction acts downward on the footing and remains constant. Secondly, the total earth thrust during unloading, B → C, is also caused mainly by the earth pressure acting on the right side. The wall friction of the right side acts upward on the footing and decreases rapidly. It is noteworthy that the wall friction of the left side also acts upward on the footing, which suggests that the earth pressure acting on both sides of the footing corresponds to the passive side. Finally, the total earth thrust during unloading, C → D, is caused mainly by the earth pressure acting on the left side of the footing. The wall friction of the right side tends to act downward on the footing and decreases. The wall friction of the left side acts upward on the footing and increases.

### *3.2 Shear force and lateral earth pressure acting on sidewall*

Figure 13 presents time histories of relative displacement between the ground surface and the footing, the shear force acting on front side of the footing for $t$=20–30 s. The waveform of the shear force resembles that of the relative displacement, indicating that the shear force depends on the relative displacement. The relation between the relative displacement and the sidewall friction is presented in Fig. 14. The sidewall friction ampli-

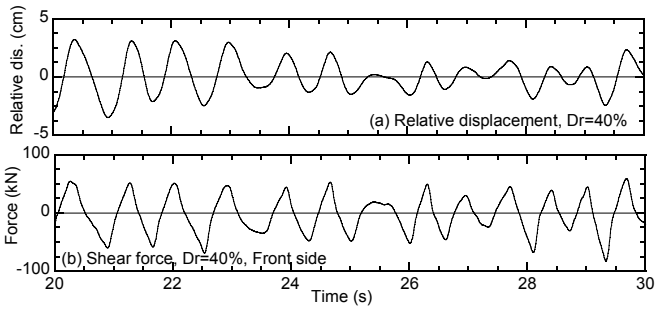


Figure 13 Time histories of relative displacement and sidewall friction

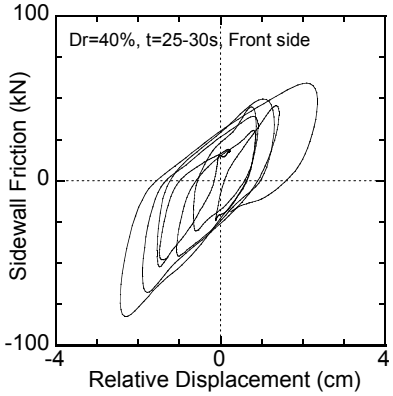


Figure 14 Relation between relative displacement and sidewall friction

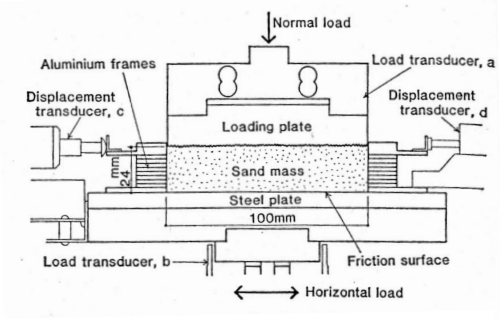


(a) Test apparatus

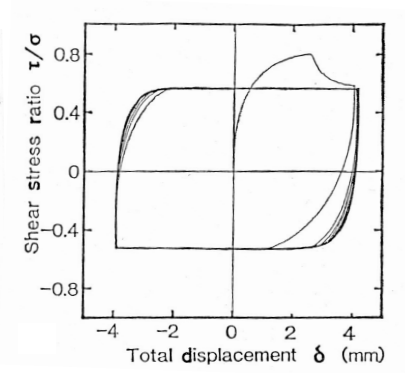


(b) Typical test results

Figure 15 Laboratory test of friction between sand and steel under repeated loading (Uesugi et al., 1998)

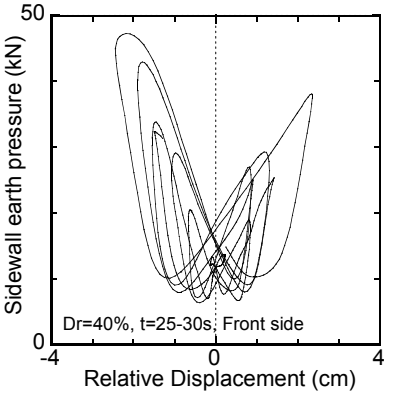


Figure 16 Relation between relative displacement and sidewall earth thrust

tude increases concomitantly with the relative displacement amplitude. A similar trend was reported by Garde and Dobry (1998) based on cyclic lateral loading centrifuge tests. Friction between sand and steel under repeated loading was investigated using laboratory tests, as presented in Fig. 15(a) under constant normal stress (Uesugi et al., 1989). Typical test results show that the shear stress ratio tends to be constant, as presented in Fig. 15(b). Figure 14 shows that this tendency differs from our experimental result.

The relation between the relative displacement and the lateral earth thrust acting on the sidewall is presented in Fig. 16 to clarify the difference between the sidewall friction based on the dynamic centrifuge test and the friction based on the laboratory test. The earth thrust amplitude increases with increasing relative displacement. Therefore, the sidewall friction amplitude increases with increasing relative displacement, as presented in Fig. 14.

## 4. CONCLUSION

Dynamic centrifuge tests on a superstructure-footing-pile model in a dry sand deposit were performed. The following conclusions were drawn.

(1) The earth pressure and wall friction acting on the active and passive sides of the footing were investigated. The hysteresis loop shape of the relative displacement and the wall friction resemble those of the earth thrust. When the total earth thrust amplitudes decreases, the wall friction of both sides tends to act upward on the footing, suggesting that the earth pressure acting on both sides corresponds to the passive side.

(2) The sidewall friction and earth pressure acting on the sidewalls of the footing were investigated. The sidewall friction amplitude increases with increasing relative displacement because the earth pressure amplitude increases with increasing relative displacement.

## REFERENCES

Gadre, A. and Dobry, R. (1998). Lateral cyclic loading centrifuge tests on square embedded footing, Journal *of Geotechnical and Geoenvironmental Engineering, ASCE*, **124, 11**, 1128-1138.

Tamura, S., Tokimatsu, K., Uchida, A., Funahara, H., and Abe, A. (2002). Relation between seismic earth pressure acting on embedded footing and inertial force based on liquefaction test using large scale shear box, *Journal of Struct. Constr. Eng., AIJ*, **559**, 129-134. (in Japanese)

Tamura, S. and Tokimatsu, K. (2005). Seismic earth pressure acting on embedded footing based on large-scale shaking table tests, Geotechnical Special Publication, *ASCE*, **145**, 83-96.

Tamura, S., Imayoshi, T. and Sakamoto T. (2007). Earth pressure and sidewall friction acting on an embedded footing in dry sand based on centrifuge tests, *Soils and Foundations, Japan Geotechnical Society*, **47**(4), 811-819.

Uesugi, M., Kishida H and Tsubakihara Y. (1989). Friction between sand and steel under repeated loading, *Soils and Foundations*, *Japan Geotechnical Society,* **29**(3), 127-137.